Title

Interconnection of Key Microbial Functional Genes for Enhanced Benzo[a]pyrene Biodegradation in Sediments by Microbial Electrochemistry



Journal

Environmental Science and Technology, 51(15)

ISSN

0013-936X

Authors

Yan, Zaisheng

He, Yuhong

Cai, Haiyuan

et al.

Publication Date

2017-08-01

DOI

10.1021/acs.est.7b00209

Peer reviewed

# Interconnection of Key Microbial Functional Genes for Enhanced Benzo[*a*]pyrene Biodegradation in Sediments by Microbial Electrochemistry

Zaisheng Yan,[†] Yuhong He,[†] Haiyuan Cai,[†] Joy D. Van Nostrand,[‡] Zhili He,[‡] Jizhong Zhou,[‡,§,∥] Lee R. Krumholz,[‡] and He-Long Jiang*[,†]

† State Key Laboratory of Lake Science and Environment, Nanjing Institute of Geography and Limnology, Chinese Academy of Sciences, Nanjing 210008, China

‡ Department of Microbiology and Plant Biology, University of Oklahoma, Norman, Oklahoma 73019, United States

§ Earth Sciences Division, Lawrence Berkeley National Laboratory, Berkeley, California 94720, United States

∥ Department of Environmental Science and Engineering, Tsinghua University, Beijing 100084, China

Corresponding Author * e-mail: hljiang@niglas.ac.cn (H.L.J.).

Abstract

Sediment microbial fuel cells (SMFCs) can stimulate the degradation of polycyclic aromatic hydrocarbons in sediments, but the mechanism of this process is poorly understood at the microbial functional gene level. Here, the use of SMFC resulted in 92% benzo[*a*]pyrene (B*a*P) removal over 970 days relative to 54% in the controls. Sediment functions, microbial community structure, and network interactions were dramatically altered by the SMFC employment. Functional gene analysis showed that *c*-type cytochrome genes for electron transfer, aromatic degradation genes, and extracellular ligninolytic enzymes involved in lignin degradation were significantly enriched in bulk sediments during SMFC operation. Correspondingly, chemical analysis of the system showed that these genetic changes resulted in increases in the levels of easily oxidizable organic carbon and humic acids which may have resulted in increased B*a*P bioavailability and increased degradation rates. Tracking microbial functional genes and corresponding organic matter responses should aid mechanistic understanding of B*a*P enhanced biodegradation by microbial electrochemistry and development of sustainable bioremediation strategies.

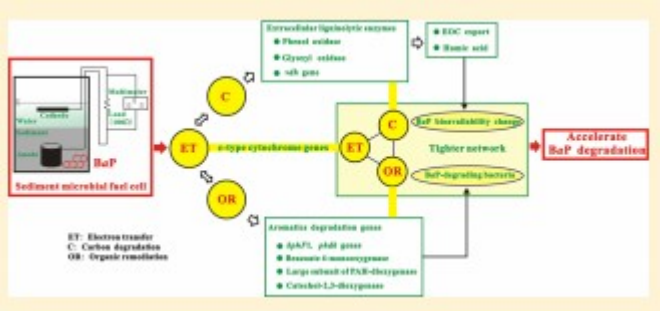


Introduction

Polycyclic aromatic hydrocarbons (PAHs) are ubiquitous environmental pollutants and pose a serious risk for both humans and ecosystems in which they are present.(1, 2) In aquatic environments, PAHs generally accumulate in sediments due to their strong hydrophobicity.(3) High molecular weight (HMW) PAHs, such as benzo[*a*]pyrene (B*a*P), a five-ring compound, shows carcinogenicity, teratogenicity, and acute toxicity.(4, 5) Thus, removal of HMW-PAHs from contaminated sediments is becoming increasingly important to mitigate the associated risks.

PAHs, once entering into sediments, are subject to natural attenuation which involved biotic/abiotic degradation.(4) Microbial degradation under aerobic or anaerobic condition by microbes represents the major mechanism for the ecological recovery of PAHs-contaminated sites.(2, 6-8) Even so, PAHs often persist as contaminants in sedimentary anoxic environments because of a lack of suitable electron acceptors.(9, 10)

To facilitate PAHs removal from sediments, biostimulation techniques involving addition of electron acceptors such as oxygen, nitrate, sulfate, ferric iron, or an electrode serving as the electron acceptor have been proposed.(9, 11, 12) The anode of the sediment microbial fuel cell (SMFC) as an electron acceptor for stimulating the degradation of aromatic hydrocarbon contaminants could be useful as it provides a low-cost, low-maintenance, and continuous sink for electrons.(9, 10) Previous studies have been successful using an electrode approach to improve the removal of hydrocarbons including diesel,(13, 14) petroleum,(15) petroleum sludge,(16) or PAHs.(2, 10)

The SMFC has been shown to alter the microbial community on the anode surface, and those distinctive microbial communities enriched on the anode biofilm played a key role in SMFC enhancement of PAH bioremediation.(2, 14) However, it was still unknown how SMFC operation affected microbial functional structures and its possible relationship with the biogeochemical cycle in the bulk sediments during enhanced degradation of HMW-PAHs. The genetic determinants of all these processes and the mechanisms involved in their regulation are much less studied.

Within sediments, organic matter (OM) was an important factor influencing the degradation of PAHs.(3, 17) Many studies have shown that the

bioavailability of PAHs was controlled by the interaction between PAHs and sediment OM.(3, 17-19) Complex components of sediment OM have different effects on PAHs transformation in sediments. For example, labile OM such as cyanobacteria-derived OM could dramatically enhance pyrene and B*a*P degradation, which was related to higher bioavailability and PAH-degrading bacteria number with a result of biostimulation and priming effect by labile carbon.(3, 20)

The electrode-driven microbial process not only altered sediment OM characteristics, but also enhanced the decomposition of OM.(21, 22) It was found that sediment OM around the electrodes had an increased level of aromatics with a higher humic acid (HA) fraction, a larger molecular size, and index of humification.(10, 21) The presence of dissolved OM such as HA is currently considered a valid biostimulation strategy to speed up PAHs bioremediation.(23, 24) However, the effect of HA on degradation of PAHs in sediments depended on the exposure regime.(25) HA could lower biodegradation via binding between PAHs and HA, but also might act as carriers of PAH compounds to induce PAHs flux to the degrading bacteria.(25, 26) Additionally, HA can serve as an electron acceptor and redox mediator for microbial respiration in sediments.(27) So, the role of HA in HMW-PAHs biodegradation is complex.

In this study, we hypothesized that (1) SMFC employment will influence the interactions of microbial functional groups in bulk sediments; and (2) carbon cycling and organic remediation functional genes in sediments will be enriched during SMFC use and closely related to B*a*P biodegradation. To test these hypotheses, both GeoChip and community sequencing were used to analyze functional genes and microbial community structures involved in organic carbon transformation and bioremediation. GeoChip 5.0 contains about 167 000 50-mer oligonucleotide probes covering ~395 000 coding sequences from >1590 functional genes involved in carbon cycling, organic remediation, electron transfer, and other environmental processes,(28) and allows us to analyze the functional composition, structure, and dynamics of microbial communities.

## Materials and Methods

### Sediment and Water Samples

Surface sediments (at 0–10 cm depth) and overlying water were collected from East Taihu Lake (30°58′ N, 120°22′ E) in China, and transported to the laboratory immediately. After sieving at 2 mm, bulk samples of surface sediment were mixed and homogenized. B*a*P was added to the sediments by mixing a stock solution (1000 mg $L^{-1}$ of B*a*P in acetonitrile; 98% purity, Alfa Aesar Co., U.K.), with wet sediments followed by mechanical mixing(2, 3) to a final concentration of B*a*P of 1000 μg $kg^{-1}$ dry sediments, much higher than the probable effect level (PEL) according to sediment quality guidelines.(29) The cosolvent acetonitrile was allowed to maximize removal by volatilization in the fume hood.

## Experimental Design and Sampling Procedures

Plexiglas columns with approximately 4-L volume (12 × 35 $cm^2$, diameter × height) were used as sediment microcosms to perform the biodegradation experiments in the dark at 25 °C. Each microcosm contained 1600 g wet sediment and 1.2 L surface water. SMFCs were installed in the sediment microcosms as described in previous studies.(2, 10, 30) The anode composed of a graphite felt cylinder (6.4 × 8 × 0.5 $cm^3$, diameter × height × thickness) was buried 5 cm below the sediment surface. The cathode, composed of round graphite felt (9.5 × 0.5 $cm^2$, diameter × thickness), was placed 6 cm above the sediment in the water column, and the overlying water was continuously bubbled with air to maintain dissolved oxygen concentration above 5 mg $L^{-1}$. All connections were made with water-tight connectors using marine-grade wire and sealed with silver conductive epoxy and marine epoxy. The voltage signal between the anode and cathode across an external load of 100 Ω was measured using a multimeter (model 2700, Keithley Instruments, Cleveland, OH, U.S.A.). Details of electrochemical measurement and SMFC performance are described in the Supporting Information (SI). In addition, the control treatment was applied to determine natural attenuation of B*a*P in sediment without SMFC employment. Each experimental condition was performed in triplicate.

During experiments, sediment samples (10 g) were taken from each microcosm at days 60, 90, 180, 450, and 970. The following physical and chemical parameters were measured: B*a*P, easily oxidizable organic carbon (EOC), total carbon (TC), humic acid (HA), total nitrogen (TN), and total phosphate (TP). More detailed information on geochemical analysis and initial properties of the sediment sample are provided in SI Table S1. Aliquots (5 g) of sediment were stored at −80 °C for molecular analysis. At the end of experiments, anode biofilm samples were collected from sediment microcosms. The anode electrodes were rinsed with sterile water to remove visible sediments on the surface, and then a sterile razor blade was used to scrape the electrodes vigorously to acquire a complex consisting of carbon felt and electrode-associated microbes for subsequent DNA extraction.(2)

## DNA Extraction, 454 Pyrosequencing, and GeoChip Hybridization

Sediment DNA for 454 pyrosequencing was extracted with a PowerSoilDNA Isolation Kit (MO BIO) according to the manufacturer’s instructions. DNA quality was assessed by 260 nm/280 nm and 260/230 nm ratios, and DNA concentration was estimated with a Nanodrop 2000 spectrophotometer (NanoDrop Technologies, Wilmington, U.S.A.). Roche GS-FLX 454 pyrosequencing was conducted by Meiji Biotechnology Company (Shanghai, China). Nucleotide sequences were all deposited in the GenBank database (accession number: SRP109064). Details of amplicon preparation, sequencing and data analysis are described in the SI.

Sediment DNA for GeoChip analysis was extracted using a freeze-grinding mechanical lysis approach in order to get a large fragment of DNA for direct

hybridization as described previously.(31) GeoChip 5.0 was synthesized by Agilent (Santa Clara, CA, U.S.A.) and used to analyze the functional structure of the microbial communities and functional gene abundances. Signal intensities were measured on the basis of scanned images. A floating signal-to-noise ratio was used so that thermophile probes accounted for 5% of the positive probes. Details for template amplification, labeling and hybridization, image processing and GeoChip data preprocessing are described in the SI.

B*a*P Bioavailability and Enumeration of PAH-Degrading Microorganisms

An aqueous-based mild extraction technique utilizing hydroxypropyl-β-cyclodextrin (HPCD) was adapted to evaluate the change of PAHs bioavailability in sediments,(3) and HA-binding experiments (binding isotherms) were performed with a fixed HA concentration of 25 mg $L^{-1}$ and increasing PAH concentrations from 0 to 75% of their water solubility, as described in a previous report with a slight modification(23) and additional details provided in the SI.

Bacterial counts from triplicate bulk sediment samples were performed using a most probable number (MPN) method,(2) with details for aerobic and anaerobic cultivation provided in the SI.

Network Construction and Network Characterization Analysis

To understand the interactions among different microbial communities and their responses to SMFC addition, a random matrix theory (RMT)-based approach was used to discern functional and phylogenetic molecular ecological networks (f/pMENs) in sediment microbial communities based on GeoChip data and community sequence data.(32) The data sets were uploaded to the open-accessible network analysis pipeline (Molecular Ecological Network Analysis Pipeline, MENAP, http://ieg2.ou.edu/MENA), and the networks were constructed using random matrix theory (RMT)-based methods.(33)

Cytoscape 3.2.1 software was used to visualize the network graphs.(33) Other information about genes, e.g., taxonomy, relative abundance, and edge information, e.g., weights and positive and negative correlations, was also imported into the software and visualized in the network figures. Since we are interested in the impact of SMFC employment on network interactions, the f/pMENs were constructed separately for the SMFC treatment and control treatments. Various indexes, including average degree (connectivity), nodes, edges, average clustering coefficient, average geodesic distance, and modularity were used to describe the properties of individual nodes in the network and the overall topologies or structures of the different networks.

## Statistical Analysis

Preprocessed data (e.g., GeoChip, 454 pyrosequencing) were analyzed as follows: (1) microbial diversity index using the two-tailed *t*-test; (2) hierarchical clustering for microbial community structure and composition; (3) analysis of similarity, permutational multivariate analysis of variance using distance matrices and multiresponse permutation procedure analysis of difference of microbial communities; (4) percentage change of functional genes within SMFCs were calculated using the following formula: $(T_S\text{-}T_C) \times 100/T_C$, where $T_C$ and $T_S$ were the average signal intensities of genes detected by GeoChip 5.0 in the control treatment samples and the SMFC treatment samples, respectively; and (5) Mantel and redundancy analysis and the corresponding partial analyses, were used to link the functional structure of microbial communities with environmental variables.

## Results

### Effects of SMFC Employment on Sediment Chemical Properties

During 970 days of biostimulation, the sediment B*a*P content was significantly decreased ($P < 0.01$) from 935.2 μg $kg^{-1}$ dry sediment to 74.7 μg $kg^{-1}$ dry sediment in the SMFC treatment (92% loss), compared to 54.2% B*a*P removal in the control due to natural attenuation (Figure 1).

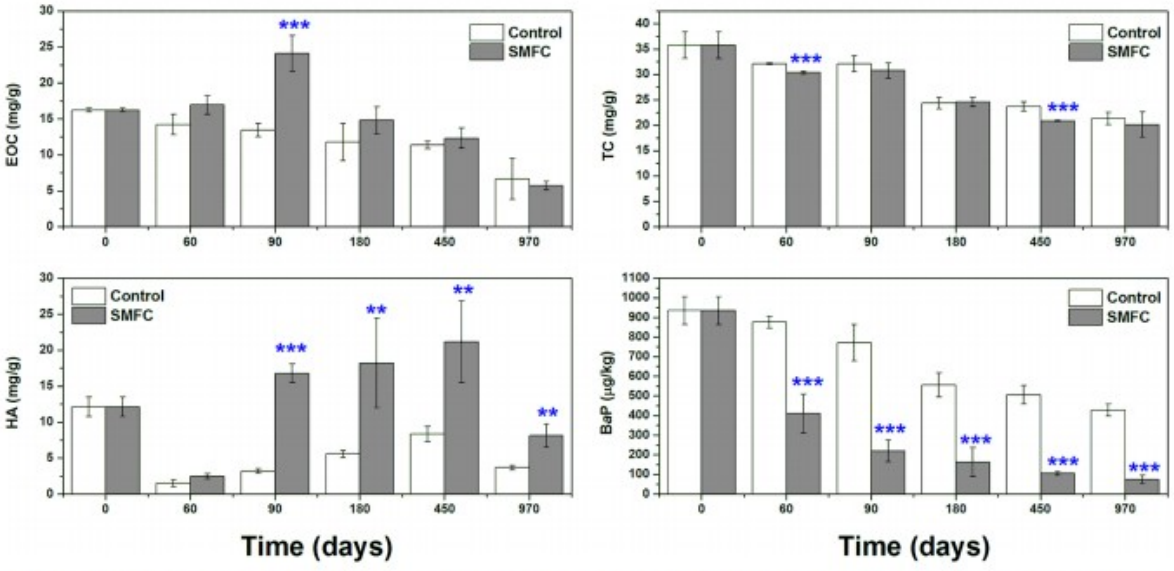


**Figure 1.** Major geochemical properties (EOC: easily oxidizable organic carbon; TC: total carbon; HA: humic acid; B*a*P: benzo[*a*]pyrene) of the sediments. Significances between the samples from the SMFC and control treatments were performed by the Student *t*-test. $^{***}p < 0.01$;$^{**}p < 0.05$.

The SMFC treatment caused EOC to rise between days 60 and 90 and then decrease through the end of the experiments, whereas the EOC content of the control decreased gradually during the entire experimental period (Figure 1). However, the HA concentration increased until day 450 in both treatments and then decreased at the 970 day time point. EOC concentration on day 90 and HA on days 90, 180, 450, and 970 were significantly ($p <$

0.05) higher in the SMFC treatment. These results indicate that sedimentary and/or refractory organic carbon degradation was stimulated by the SMFC.

The HA content decreased sharply at the beginning of the experiments, and was lowest on day 60 in all treatments (Figure 1). After that, the HA content in the controls increased slowly to 8.3 ± 1.1 mg DW $g^{-1}$ DW sediment on day 450, and then decreased to day 970. In comparison, HA content in sediments in SMFC treatment increased to a much higher level (21.2 ± 5.7 mg DW $g^{-1}$ DW) sediment on day 450, and then decreased to day 970. After day 60, the HA content in sediments in SMFC treatment was more than double those in the control.

Overall Responses of Sediment Microbial Communities to SMFC Employment

To determine the overall response of sediment microbial communities to SMFC operation, the microbial communities in the sediment within the SMFC and control treatments were analyzed with (1) functional gene arrays (i.e., GeoChip), which measure the function and composition of microbial communities, and (2) 16S rRNA gene-based pyrosequencing, which assesses the phylogenetic composition of microbial communities. Although no significant difference was detected in the overall microbial diversity, measured as the number of functional genes or OTUs, Shannon, Simpson, or Chao1 index (Table S2), the microbial functional gene diversity on day 90 and the microbial community diversity on day 180 were significantly ($p < 0.05$) different between the control and SMFC treatments. Significantly more functional genes ($p < 0.05$) were detected in the SMFC samples than in the control on day 90. The microbial functional diversity based on Shannon ($H'$) and Simpson's ($1/D$) indices was also significantly ($p < 0.01$) higher in the SMFC treatment samples on day 90. However, significant ($p < 0.05$) decreases in microbial community diversity based on Shannon ($H'$) and Chao1 indices were observed in the SMFC treatment samples on day 180. In addition, the overall microbial community functional structure in the SMFC treatment was significantly ($p < 0.05$) different from the control treatment as revealed by three nonparametric multivariate statistical tests: MRPP, ANOSIM, and Adonis (Table S3) based on GeoChip 5.0 analysis of all detected functional genes. Furthermore, the community functional structures at the different treatment time points were also significantly ($p < 0.05$) different based on the Adonis test.

Analysis of 16S rRNA gene amplicon sequences showed that the abundance of five phyla (*Firmicutes*, *Proteobacteria*, *Actinobacteria*, *Bacteroidetes*, and *Nitrospirae*) markedly increased in the SMFC treatment sediments (Figure 2A). At the genus level, however, 24 genera from dominant phyla had altered abundances in the SMFC treatment sediments with *Bacillus*, *Pseudomonas*, and *Clostridium* clearly increased on day 180 (Figure 2C). Microbial communities from the control and SMFC treatments formed different clusters in hierarchical clustering based on community (Figure 2B) and functional gene analysis (Figure S1). Interestingly, most of the genera

detected (Figure 2D) are known to be metabolically versatile and could be involved in multiple biogeochemical cycling processes. For example, the gene families detected from genera *Bacillus*, *Burkholderia*, *Clostridium*, *Geobacter*, *Mycobacterium*, *Nocardia*, *Pseudomonas*, and *Rhodococcus*, are involved in carbon-cycling (C) and organic remediation (OR) processes. The anaerobic genus *Desulfobacca* (Figure 2C) substantially enriched in the bulk sediment in SMFC treatment on day 450 are also involved in carbon degradation processes. The gene families from *Burkholderia*, *Geobacter*, and *Pseudomonas* are also involved in electron transfer (ET) processes. The average functional gene abundances from microorganisms increased between 1 and 17 times within the initial 60 days following SMFC employment (Figure 2D).

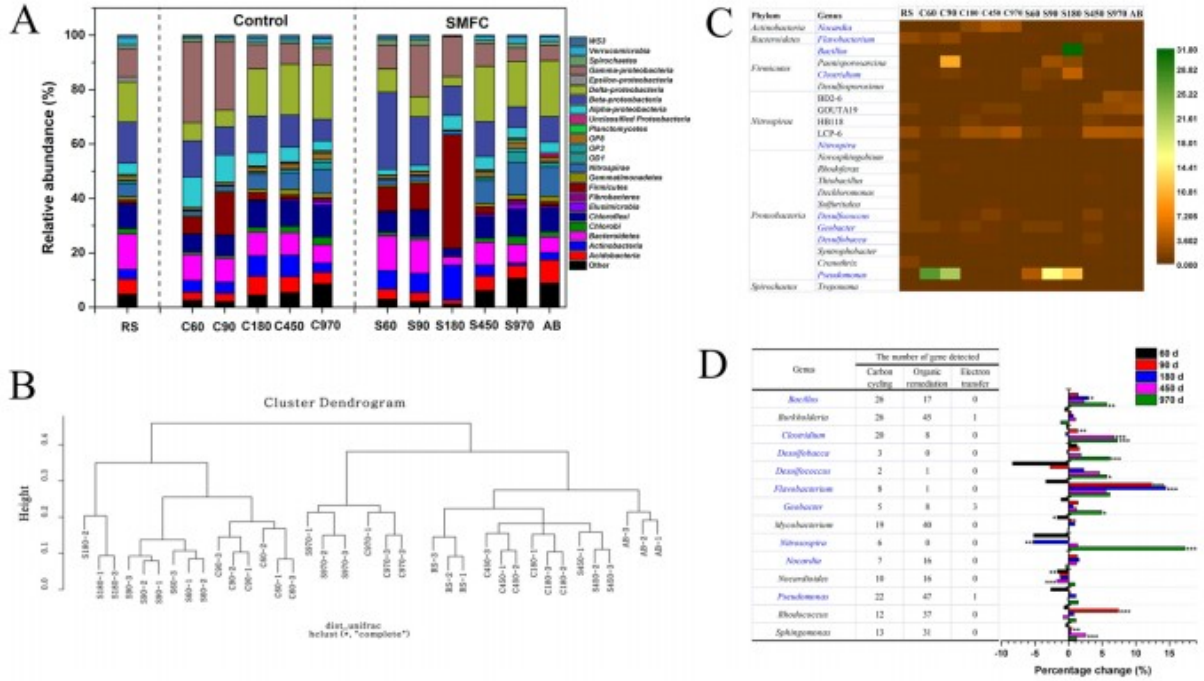


**Figure 2.** Relative abundance of bacterial phylogenetic groups at the phylum level (A), clusters of the bacterial communities of sediment samples and anode biofilms (B), the heat map at the genus level (C) based on 454 pyrosequencing, and the commonly significantly increased functional genes from the microorganisms with metabolic versatility (D). The genera that are less than 1% of total composition in all libraries were not included in the heat map. The calculation of percentage change was based on the average signal intensity of each microorganism. The same genus based on 454 pyrosequencing (C) and functional genes from the microorganisms with metabolic versatility (D) were marked with blue. (RS: Raw sediment; C: Control; S: SMFC; AB: Anode biofilms.).

The methanogen community based on genus revealed that the dominant methanogen genera in bulk sediments were *Methanosaeta*, *Candidatusmethanoregula*, *Methanosarcina*, and *Methanolinea* (Figure S8). The results clearly showed that the abundance of *Methanosaeta*, *Candidatus methanoregula*, and *Methanosarcina* in bulk sediments in the SMFC at the end of experiments was substantially lower than those in the control sediments, which suggested that SMFC might play a role in affecting the microbial metabolism in sediments and inhibit methanogenic activity to some extent.

## Impact of SMFC Employment on the Architecture of Functional and Phylogenetic Molecular Ecological Networks (f/pMENs)

Network indexes were calculated separately for both f/pMENs under the SMFC and control treatments (Figure 3 and Table S4). The harmonic geodesic distance (GD) value was close to the logarithm of the total number of network nodes, suggesting that the fMEN had the typical property of small world. The modularity value was significantly higher than the *M* value from the corresponding randomized networks. Therefore, this fMEN appeared to be modular. Moreover, the network structures of these two microbial communities involved in carbon cycling, organic remediation, and electron transfer functional genes were distinct according to significantly different ($p < 0.001$) indices between SMFC and control treatments during the 180 days of the experiments (Figure 3). Interestingly, compared to the control, the fMENs in the SMFC treatment generally had higher connectivity, shorter path lengths, higher clustering efficiencies, and more modules (Figure 3), which are key network properties in terms of system efficiency and robustness. All of the above results suggested that SMFCs could have a substantial impact on the architecture of the fMENs in the microbial communities during 180-day experiments. Various network indices were also calculated separately for both f/pMENs under the SMFC and control treatments during the overall and 180 days of the experiment (Table S4). The average geodesic distance, average clustering coefficient, and modularity (as well as many other network parameters) of these f/pMENs were considerably different between the SMFC treatment and the control. These findings suggest that the fMENs of microbial communities (carbon cycling, organic remediation and electron transfer) in the SMFC treatment has a tighter network (more modules, higher connectivity and higher clustering efficiencies), implicating stronger coupling between microbes in mediating PAH degradation and extracellular electron transfer compared to the control during the 180 days of the experiments.

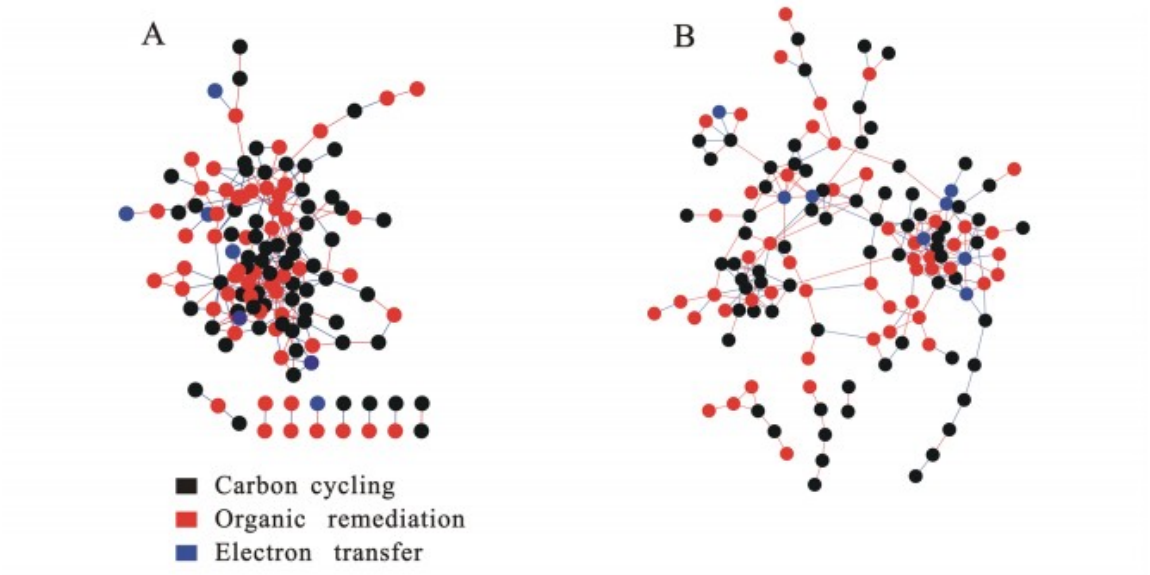


C

| Community | Empirical networks | | | | | | | | Random networks | | |
|---|---|---|---|---|---|---|---|---|---|---|---|
| | Nodes (S) | Edges (L) | L/S | $L/S^2$ | Avg connectivity (avgK) | Average geodesic distance (GD) | Average clustering coefficient (avgCC) | Modularity (no. of modules) | Average geodesic distance (GD) | Average clustering coefficient (avgCC) | Modularity(M) |
| SMFCs (A) | 130 | 249 | 1.92 | 0.0147 | 3.831 | 3.72 | 0.293 | 0.593 (17) | 3.339±0.171 | 0.048±0.013 | 0.468±0.026 |
| Control (B) | 132 | 240 | 1.82 | 0.0137 | 3.636 | 4.64 | 0.285 | 0.712 (10) | 3.701±0.173 | 0.033±0.012 | 0.502±0.012 |

**Figure 3.** Modular organization of the fMENs of microbial communities (carbon cycling, organic remediation and electron transfer) in the SMFC treatment (A) and control treatment (B) during 180-day experiment, and major topological properties (C) of the empirical fMENs of microbial communities in the SMFC (A) and control treatments (B) and their associated random fMENs during 180-day experiment. Colors of the nodes indicate different functional categories. Clear modular architecture was observed in this fMENs. Each node signifies a microorganism that carried out certain ecological function detected by GeoChip. A blue line indicates a positive interaction between two individual nodes, while a red line indicates a negative interaction.

## Responses of Microbial Functional Genes to SMFC Employment

Microbial functional genes detected for main biogeochemical/metabolic processes are listed in Table S5. Functional genes involved in carbon degradation and organic contaminant degradation were most abundant in major biogeochemical/metabolic processes. Overall, 16% and 9% of the detected gene variants were involved in carbon metabolism and organic contaminants degradation, respectively.

### *Electron Transfer Genes*

Among the detected genes involved in electron transfer, the relative abundances of *c*-type cytochrome $c_2$ genes showed significant ($p < 0.05$) increase on days 60 and 90 after the SMFC operation (Table S6). All *c*-type cytochrome $c_2$ genes were derived from the organism *Dechloromonas aromatica* RCB (Figure S3), which was capable of anaerobic degradation of aromatic hydrocarbon and benzene.(7, 34) In addition, the abundances of *c*-type cytochrome, cytochrome $c_1$, and cytochrome $c_6$ genes were also significantly ($p < 0.05$) enriched on day 450 or day 970 after SMFC employment. The cytochrome genes and *c*-type cytochrome genes were detected in the sediments from *Geobacter*, *Shewanella*, *Pseudomonas*, *Desulfovibrio*, *Anaeromyxobacter*, and *Rhodobacter* in the SMFC and control

treatments at different time points (Table S7). And the abundances of *c*-type cytochrome genes from these important genera were also significantly ($p < 0.1$) enriched from day 60 to day 970 at different time points after SMFC employment. Significant differences in signal intensities were not observed for hydrogenase genes and P450 genes between the SMFC and control treatments.

*Carbon-Cycling Genes*

Among the 11 655 C-cycling genes detected, 69.5% of them were involved in C compound degradation, such as cellulose, chitin, hemicelluloses, and lignin, which are the most abundant carbon sources derived from plant tissues or organisms in lake ecosystems. Most of these genes showed significantly ($p < 0.05$) higher abundance on days 90 and 970 after SMFC employment (Table S8). The two genes about *endopolygalacturonase* and *exopolygalacturonase* enzymes for complex polymer degradation showed significant increase in the SMFC treatment on day 60. In addition, enriched genes for complex polymer degradation were also observed in the SMFC treatment at the other time points. In addition, the glyoxyl oxidase and phenol oxidase enzymes and *vdh* gene (encoding vanillin dehydrogenase) showed significant ($p < 0.05$) increase in the SMFC treatment on day 90 (Figure 4). These types of genes enriched at different time points could also be important in degradation of refractory organic carbon, such as lignin, PAH, and their intermediates.(35, 36)

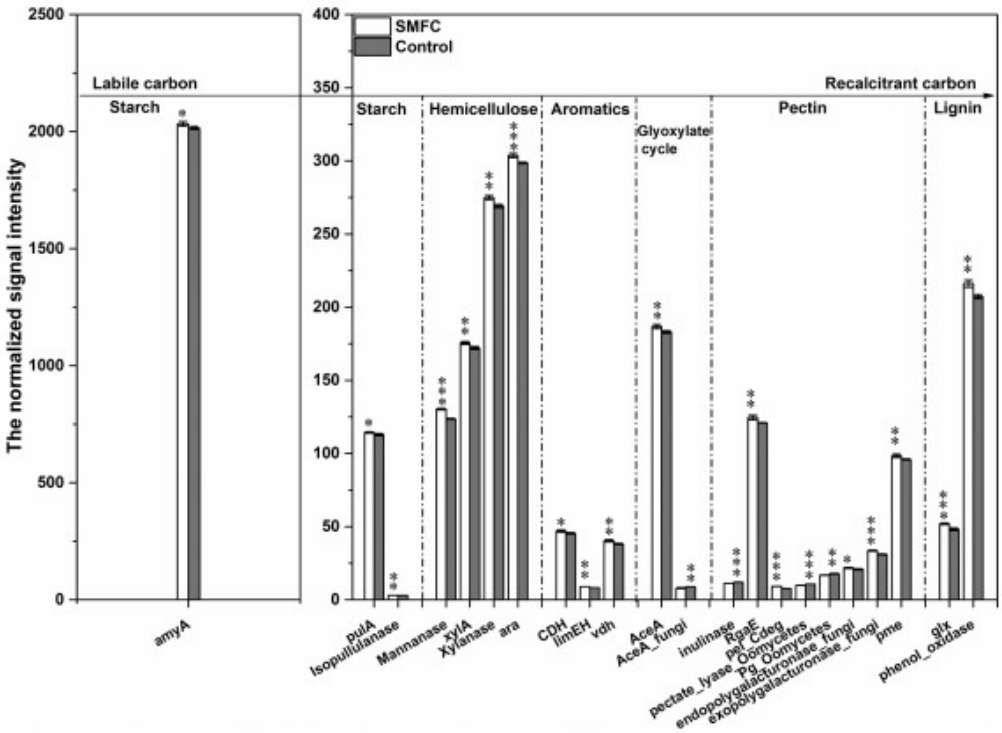


**Figure 4.** Normalized signal intensity of the detected key functional gens involved in carbon degradation on day 90. Significances between the samples from the SMFC and control treatments were performed by the Student *t*-test. ***$p < 0.01$;**$p < 0.05$;*$p < 0.1$.

## *Organic Contaminant Degradation Genes*

A total of 6169 gene sequences from 98 gene families involved in organic contaminant degradation showed positive hybridization signals. Hierarchical clustering analysis was performed on all degradation genes (Figure S2). All of the samples with the SMFC treatment on days 60, 90, 180, and 450 grouped together, indicating that the microbial communities presented similar functional patterns in organic contaminant degradation. These organic contaminant degradation genes involved in aromatics degradation, BTEX, and related aromatics degradation, nitroaromatics, chlorinated solvents, and PAHs degradation were significantly ($p < 0.05$) enriched at different time points after SMFC employment (Table 1).

**Table 1. Effects of SMFC Employment on Abundances of Key Functional Genes Involved in Organic Remediation Genes**

| | | percentage change (%)[a] | | | | | *p*-value[b] | | | | |
|---|---|---|---|---|---|---|---|---|---|---|---|
| gene or enzyme | functional process | 60 d | 90 d | 180 d | 450 d | 970 d | 60 d | 90 d | 180 d | 450 d | 970 d |
| bph | aromatic carboxylic acid | −3.61 | 10.76 | 6.48 | 10.10 | 7.02 | 0.3986 | **0.0052** | 0.2345 | 0.1181 | 0.3215 |
| mhpA | aromatic carboxylic acid | 4.01 | −1.34 | −1.67 | −2.55 | 2.52 | 0.1989 | 0.3225 | 0.5255 | 0.1770 | **0.0060** |
| phtA | aromatic carboxylic acid | −0.40 | −3.17 | −1.88 | 3.81 | −0.75 | 0.7080 | 0.0732 | 0.2763 | **0.0065** | 0.6733 |
| pchCF | BTEX and related aromatics | −6.12 | −0.22 | 2.04 | 2.61 | 7.37 | 0.0586 | 0.6319 | 0.3631 | 0.0766 | **0.0433** |
| tutFDG | BTEX and related aromatics | −0.17 | −2.29 | −1.78 | 12.35 | 3.50 | 0.9690 | 0.2951 | 0.4106 | **0.0066** | 0.3791 |
| HBH | BTEX and related aromatics | −3.59 | 0.82 | 6.34 | −1.23 | −0.13 | 0.1661 | 0.5987 | **0.0080** | 0.6260 | 0.9676 |
| bbs | BTEX and related aromatics | −0.67 | 0.70 | 0.11 | 1.05 | 1.07 | 0.2390 | 0.0673 | 0.9414 | 0.1332 | **0.0334** |
| rd | chlorinated solvents | −0.10 | 4.77 | −4.07 | 1.45 | 2.58 | 0.9625 | **0.0418** | 0.1985 | 0.2970 | 0.0668 |
| bphF1 | polycyclic aromatics | −1.97 | 1.22 | 3.24 | 1.12 | 0.80 | 0.3686 | 0.4299 | **0.0020** | 0.3327 | 0.6653 |
| phdk | polycyclic aromatics | −8.54 | 14.46 | −2.20 | 1.67 | −5.22 | 0.1850 | **0.0500** | 0.8040 | 0.7410 | 0.2990 |
| qorl | polycyclic aromatics | −0.38 | −0.29 | −0.42 | 0.55 | 0.63 | 0.2310 | 0.3909 | 0.6084 | 0.3979 | 0.2746 |
| nbaC | nitroaromatics | −5.61 | −3.68 | 4.51 | 2.93 | 14.00 | 0.1218 | 0.3466 | 0.0886 | 0.3136 | **0.0020** |
| nitroreductase_b | nitroaromatics | −1.19 | 3.22 | 3.29 | −0.28 | 2.78 | 0.2826 | **0.0003** | 0.2286 | 0.8149 | 0.3317 |
| oxdB | nitroaromatics | 7.82 | −0.94 | 4.33 | −1.08 | 11.19 | **0.0187** | 0.6682 | 0.2370 | 0.5578 | **0.0020** |
| amiE | other aromatics | 0.06 | 2.58 | 0.94 | −2.29 | −1.86 | 0.9775 | **0.0002** | 0.6389 | 0.3525 | 0.6939 |
| catechol-2,3-dioxygenase | other aromatics | −0.37 | 2.48 | 1.16 | −1.86 | 3.77 | 0.8196 | **0.0027** | 0.3282 | 0.2202 | **0.0015** |
| nitrilase | other aromatics | −4.37 | 2.93 | 0.64 | 2.63 | 2.22 | 0.1719 | **0.0031** | 0.7569 | 0.1291 | 0.2069 |
| xln *D* | other aromatics | 4.26 | 5.31 | −0.41 | −4.54 | 11.74 | 0.3631 | 0.1587 | 0.9291 | 0.1774 | **0.0072** |
| large subunit of PAH-dioxygenase | other aromatics | 1.18 | 2.66 | 1.80 | 1.77 | −0.54 | 0.4369 | **0.0181** | 0.3189 | 0.1403 | 0.6803 |
| alkB | other hydrocarbons | −1.23 | 2.50 | −0.10 | 2.88 | 3.57 | 0.4870 | **0.0039** | 0.9132 | 0.1166 | 0.0966 |
| assA | other hydrocarbons | −3.87 | 0.60 | −4.85 | 2.05 | 18.38 | 0.4327 | 0.4398 | 0.3002 | 0.5613 | **0.0137** |
| cpnA | other hydrocarbons | −0.06 | 0.00 | −2.89 | −0.53 | 7.04 | 0.9727 | 0.9985 | 0.1114 | 0.7409 | **0.0001** |
| adpB | pesticides related compound | 0.21 | 1.92 | −0.99 | 0.95 | 1.73 | 0.6504 | 0.6634 | 0.2180 | **0.0292** | 0.4278 |

[a]Percentage change of functional genes were calculated using the following formula: $(T_S - T_C) \times 100/T_C$, where $T_C$ and $T_S$ were the average signal intensities of genes detected by GeoChip 5.0 in the control treatment samples and the SMFC treatment samples from different time points. [b]*p*-values were the Student *t*-test results between the samples from the SMFC and control treatments at different time points. The bold *p*-values indicate significant ($p < 0.05$) changes. A bold *p*-values indicates a positive percentage change between two treatments.

## *Aromatics Degradation Genes*

In total, 4408 genes involved in aromatic hydrocarbon degradation showed positive hybridization signal intensity. There were 694 aromatic carboxylic acid degradation genes detected in 11 gene families. Within the gene families detected, 3 of them (*bph*, *mhpA*, and *phtA*) increased significantly ($p < 0.05$) on days 90, 450, and 970 after SMFC employment (Table 1). Significant ($p < 0.05$) increases were observed in *bph* encoding benzoate 4-monooxygenase genes on day 90 involved in the degradation pathway of benzoyl-CoA, the most common intermediate in the anaerobic degradation of aromatic compounds.(37) The *mhpA* (229591541, 119899970, and 403195534) and *phtA* genes (118759687) with increasing signal intensity after SMFC employment, all were from bacteria *Pseudomonas* sp., *Azoarcus*

sp., *Escherichia* sp., and *Sphingomonas wittichii* RW1 (Table S9). The *mhpA* and *phtA* genes from these organisms were involved in anaerobic degradation of toluene, ethylbenzene, and naphthalene.(12, 38)

There were 284 genes from 11 gene families detected for BTEX and related aromatics degradation in all the time points after SMFC operation. Within 11 gene families detected, four of them (*pchCF* encoding p-cresol methylhydroxylase subunits, *tutFDG* encoding benzylsuccinate synthase subunits, *bbs* encoding putative E-phenylitaconyl-CoA hydratase, and *HBH* encoding hydroxybenzoate hydroxylase) showed a significantly ($p < 0.05$) higher abundance after 90-day SMFC operation with the highest in *HBH*. These genes were from bacteria, especially the important naphthalene, toluene, and ethylbenzene anaerobic degrader.(7, 12, 38) For example, the significantly ($p < 0.05$) increased *pchCF* genes (120595693) were from the facultative bacterium *Polaromonas naphthalenivorans* CJ2 and both significantly ($p < 0.1$) increased *tutFDG* (78218725) and *bbs* (56312525, 404496386) were from the important anaerobic metabolism bacteria, *Desulfovibrio desulfuricans* G20, *Azoarcus* sp. EbN1 and *Geobacter metallireducens* GS-15 (Table S9).

Also, there were 246 genes from 5 gene families detected for PAH degradation in all the time points with SMFC operation. Within 5 gene families detected, two of them (*bphF*1 and *phdk*) increased significantly ($p < 0.05$) on days 90 and 180 after SMFC employment (Table 1). Within significantly increasing genes, the *bphF*1 genes (71849040, 302863179, and 110821037) were from the *Dechloromonas aromatica* RCB, *Desulfovibrio* sp., and *Rhodococcus* sp. RHA1 (Table S9), which had been shown to be capable of anaerobic degradation of benzene, toluene, and xenobiotic compounds.(7, 37)

In addition, six genes, such as catechol encoding catechol dioxygenase, catechol-b gene encoding catechol-2,3-dioxygenase, tftH gene intradiol ring-cleavage dioxygenase, benzoate dioxygenase, ring-hydroxylating dioxygenase, and large subunit of PAH-dioxygenase were detected in all samples (Table 1). The ring-hydroxylating dioxygenase and large subunit of PAH-dioxygenase are two key PAH ring-hydroxylating dioxygenase derived from *Sphingomonas* sp. AC3 (77543319), *Sphingomonas* sp. A4 (50725019), and *Mycobacterium vanbaalenii* PYR-1 (195364366).

Catechol (encoding catechol dioxygenase) and catechol-b genes (encoding catechol-2,3-dioxygenase) are also two key dihydroxylated intermediates in PAH catabolic pathways.(39, 40) The ortho- and meta- cleavage pathways generate the tricarboxylic acid cycle intermediates originating from catechol or catechol-b genes.(40) The dioxygenase genes involved in catechol and catechol-b degradation were detected in all samples (Figure S4). The genes encoding large subunit of PAH-dioxygenase and catechol-b genes encoding catechol-2,3-dioxygenase also showed significant ($p < 0.05$) increases after SMFC operation on day 90 (Table 1).

Genes involved in the degradation of pyrene and B*a*P were also detected (Table S10). For pyrene or B*a*p catabolism, genes encoding PAH ring-hydroxylating dioxygenase large subunit derived from *Mycobacterium vanbaalenii* PYR-1 (195364366) and putative ring-hydroxylating dioxygenase derived from *Mycobacterium vanbaalenii* PYR-1 (90206044) were observed in higher abundances in the sediments with SMFC employment compared to the control at all the time points. The higher relative abundances of *Mycobacterium* based on the 16S rRNA gene sequencing in the sediments with SMFC employment were also observed compared to the control on days 60,180, and 970 (Table S10).

In total, the functional genes for aromatic carboxylic acid, BTEX, and related aromatic, catechol, and PAHs degradation in sediment were significantly enriched after SMFC employment. Moreover, most of the significantly increasing aromatics degradation genes were derived from the important anaerobic or facultative bacterial degraders.

Relationship between Microbial Functional Diversity and Environmental Variables

Redundancy analysis (RDA) was performed to identify correlations between changes in the functional gene communities after SMFC amendment and environmental variables. The relationship between the functional gene communities and the six parameters (B*a*P, EOC, TC, HA, TN, and TP) in the RDA ordination plot is shown in Figure 5. The samples from the same time points were clustered together. The first axis of the RDA explained 34.1% of the variation in functional gene communities, and was positively correlated with the TC, EOC, TP, and TN. The second axis was positively correlated with HA, but negatively correlated with B*a*P. These six geochemical parameters explained 42.2% of the total variance. Within these six parameters, the sediment TC content was identified as the most important environmental factor for shaping the functional microbial communities structure after SMFC employment through multivariate regression tree (MRT) analysis (Figure S5). The sediment HA concentration was another main environmental factor for shaping the functional microbial communities structure. In this study, key functional genes for aromatic carboxylic acid, BTEX, and related aromatics, PAH, glyoxylate cycle, cellulose, pectin, and lignin degradation were also significantly ($p < 0.05$) related with sediment TC and HA contents (Tables S11 and S12). So, the microbial community functional structure had significant relationships with sediment TC and HA dynamics.

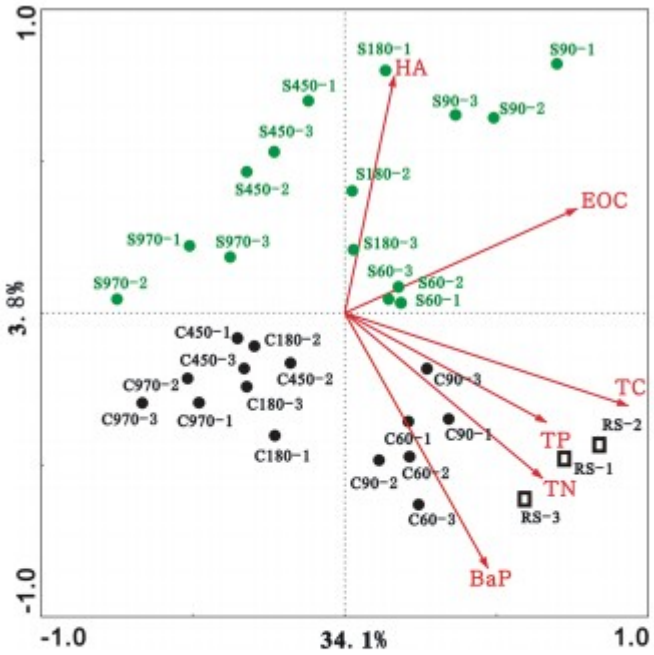


**Figure 5.** Bioplot of redundancy analysis of the functional gene communities of sediment samples from different time points. Square represent samples collected from raw sediment; black solid circles represent samples collected from the control treatments; green solid circles represent samples collected from the SMFC treatments. Descriptors (red arrows) are the concentration of six geochemical parameters (EOC: easily oxidizable organic carbon; TC: total carbon; HA: humic acid; B*a*P: benzo[*a*]pyrene; TN: total nitrogen; TP: total phosphate) in the sediment. (RS: Raw sediment; C: Control; S: SMFC).

## Bioavailability of B*a*P and PAH-Degrading Bacteria (PDB) Number

The bioavailable fractions of B*a*P were 57.69% at the beginning of experiments and progressively decreased with experiments (Table 2). The bioavailable fractions of B*a*P in the SMFC treatment were 47.23%, 46.71%, and 48.33%, which were significantly higher than those in the control treatment on days 60, 90, and 180, indicating that employment of SMFC stimulated the release of HA-binding B*a*P to the aqueous phase (Table S13), thereby increasing the B*a*P bioavailability. However, an opposite situation was observed at the end of experiments. At the end of experiments, the bioavailability for B*a*P (9.02%) in the SMFC treatment was much lower than that in the control treatment (15.03%), indicating residual B*a*P in sediments in the SMFC treatment were finally stabilized with reduced environmental risks.(41)

**Table 2. Change of B*a*P Bioavailability during the Experimental Period**

| | | BaP bioavailable fraction (%)[a] | | | | | |
|---|---|---|---|---|---|---|---|
| compound | treatment | 0 days | 60 days | 90 days | 180 days | 450 days | 970 days |
| BaP | control | 57.69 | 36.07 | 34.42 | 33.91 | 32.37 | 15.03 |
| | SMFCs | 57.69 | 47.23 | 46.71 | 48.33 | 11.24 | 9.02 |

[a]B*a*P bioavailable fraction (%) = (hydroxypropyl-$\beta$-cyclodextrin extraction amount/accelerated solvent extraction amount) × 100%

MPN-enumeration of PDB with PAH mixture (phenanthrene, pyrene, and B*a*P) or only B*a*P as the carbon source showed that the suitable degraders were present in the indigenous microbial communities in sediments (Figure S6). When using PAH mixture as carbon source, the PDB numbers in the SMFC and control treatments under anaerobic incubation condition were about ten times higher than those under aerobic condition, indicating that anaerobic biodegradation of PAHs in sediments played an important role. In addition, under both aerobic and anaerobic conditions, the numbers of PDB in sediments with the SMFC treatment showed nearly 1 order of magnitude higher than those with the control treatment regardless of using the PAH mixture or only B*a*P as carbon source.

## Operation of SMFC and Changes in Redox Potential in Sediments

SMFC operated within normal parameters throughout the experimental period, as shown by the continuous current production from SMFC (Figure S7A). The fluctuation of current output in each SMFC was observed throughout the experimental period. The fluctuation in SMFC current might be ascribed to the variation of sediment organic matter characteristics in the spiked B*a*p sediments. In addition, the changes in sampling frequency of electrical signal from once every 30 min to once every day might further weaken fluctuation. The average current in the SMFCs performed in triplicate was 0.19 ± 0.08 mA. The maximum power generation was 19.8 mW $m^{-2}$ based on anodic electrode footprint area (Figure S7B). The total coulombs were 17 444.6 coulombs at day 970. The Coulombic efficiency was estimated based on EOC removal was 19.5%. The cathode potentials were relatively constant at 345–532 mV over time. However, the anode potentials increased until day 180 and then decreased through the end of the experiments (Figure S7C). In addition, the redox potential for the SMFC in the vicinity of the anode was 132 ± 24 mV and much more than those at the same place in the control (−30 ± 13 mV). This indicates that anaerobic oxidation of organic matter occurs in the SMFC.(2, 21)

## Discussion

Microbially mediated degradation of B*a*P is a promising strategy for the potential remediation of HMW-PAHs contaminated sediments. This study found that SMFC operation altered the functional microbial community structure in bulk sediments and that resulted in the appropriate geochemical conditions for HMW-PAHs remediation.

The employment of SMFC meant the addition of one new anaerobic respiration pathway with the electrode as the electron acceptor namely electrode-reduction in sediments.(9, 10) The abundance of functional genes for aromatic hydrocarbons degradation in bulk sediments increased in the SMFC, and most of the enriched genes were from microorganisms capable of extracellular electron transfer (Table 1). Additionally, the PAH ring-hydroxylating dioxygenase large subunit and *tftH* encoding putative ring-hydroxylating dioxygenase from *Mycobacterium vanbaalenii,* were enriched

at all time points in SMFC treatment sediments. A series of enzymes from some *Mycobacterium* cultures, including those enriched above (Table S10) were shown to be responsible for pyrene and B*a*P catabolism.(40) The higher abundances of *Mycobacterium* were also found based on the 16S rRNA gene sequencing data in SMFC treatment sediments. It is therefore likely that *Mycobacterium* made a contribution to B*a*P degradation in the bulk sediments with SMFC operation. Actually, *Mycobacterium* species are promising organisms for environmental bioremediation due to their ability to catabolize aromatic compounds.(42) Moreover, the dominant genera *Bacillus*, *Clostridium*, and *Geobacter* (Figure 2C) enriched in the SMFC treatment sediments are associated with anodic electron transfer and/or anaerobic degradation of aromatic compounds.(2, 4, 7, 9)*Desulfobacca* and *Pseudomonas* found in the sediments are also important in the degradation of fluoranthene, pyrene, and B*a*P.(2, 4)

Organic pollutants can be degraded by microorganisms in sediments, but the importance of sediment OM for their transformation by specific microbial taxa is unknown.(43) The SMFC operation affected obviously the interactions of microbial populations (Table S4), and resulted in a tighter network interaction of microbial community in sediments involved in electron transfer, carbon cycling and organic remediation (Figure 3). The changes in network structure are significantly correlated with sediment TC and HA contents through multivariate regression tree (MRT) analysis (Figure S5). Additionally, the extent of B*a*P removal in the sediments was related to changes in levels of carbon cycling genes (Table S8). With SMFC operation, extracellular ligninolytic enzymes like glyoxyl oxidase, phenol oxidase, lignin peroxidase, and manganese peroxidase, were enriched (Figure 4), and these functional genes are actually involved in the degradation of recalcitrant lignin compounds as well as B*a*P degradation.(44, 45)

Furthermore, the abundance of these ligninolytic enzymes had also strong effect on the amount of sediment TC and HA in the SMFC treatments (Table S12). It follows that these enzymes enter the environment where their aggregate activity mediates key functions of carbon mineralization and humification.(36) This may explain how the mineralization of recalcitrant organic matter in the SMFC treatments would result in carbon pool transformations and then an increase in the EOC content in the sediments from day 60 to day 90 (Figure 1). As a result, B*a*P absorbed by recalcitrant organic matter would then be released, thus facilitating microbial access to B*a*P for biodegradation.(3) Also, the presence of fresh EOC in the SMFC treatment may increase degradation of the recalcitrant B*a*P in sediments through the priming effect.(3, 20)

Besides, the SMFC resulted in an increased level of HA (Figure 1). Significant ($p < 0.05$) correlations were detected by partial Mantel test between the HA content and the *vdh*, *AceA*, *pchcf*, *limeh*, and *rgl* genes for aromatic hydrocarbon or lignin degradation (Table S12). The HA fraction of sediments from the SMFC treatment had a significantly decreased PAH binding

capacity, and then led to an increase in the bioavailability of the PAH (Table S13). This likely allowed further access to PAHs for biodegradation.(26, 46, 47) It was found that even solid humic substances in sediments facilitated extracellular electron transport through a conductive network,(48) and had the added consequence of separating sites of carbon metabolism from terminal electron acceptors.(49) Currently, it was found that a diverse set of microbial communities were able to mineralize refractory OM and HMW-PAHs by extracellular electron transfer.(9) Thus, the presence of high amounts of HA increased the working efficiency of SMFC through mediating the setup of electron transfer and organic remediation. Also, a promising field application of HA amendment for increase the radius of influence (ROI) of SMFC for PAH degradation was proposed, and quantitative determination of key functional genes may be valuable as a proxy for monitoring the remediation process of contaminated sediments.(50-52)

In summary, the results allow us to form a conceptual model for understanding the interconnection of microbial functional genes for enhanced B*a*P biodegradation in sediments by microbial electrochemistry. First, SMFC employment greatly stimulated the *c*-type cytochrome genes for electron transfer within the initial 60 days. And these genes involved in electron transfer were also capable of anaerobic degradation of PAHs. After that, the aromatic degradation genes for organic remediation, genes involved in electron transfer and extracellular ligninolytic enzymes involved in lignin degradation were significantly enriched in the SMFC treatment sediments. Second, these genetic changes resulted in easily oxidizable organic carbon export, high amounts of humic acids after 60 days and B*a*P degraders increasing in bulk sediments which could increase B*a*P bioavailability and increased B*a*P degradation rates. In addition, the abundance of key genes involved in the PAH anaerobic degradation and PAH central catabolic pathways significantly increased, such as *bphF*1, genes encoding benzoate 4-monooxygenase, large subunit of PAH-dioxygenase, and catechol-b genes. Finally, cooperative interactions of functional communities of electron transfer, carbon cycling, and organic remediation in the bulk sediments accelerated B*a*P degradation.

## Acknowledgments

This work was supported by grants from National Natural Science Foundation of China (41371456, 41671496, 51379199, and 51679228), and CAS Interdisciplinary Innovation Team.

## References

(1) Liu, Y.; Beckingham, B.; Ruegner, H.; Li, Z.; Ma, L. M.; Schwientek, M.; Xie, H.; Zhao, J. F.; Grathwohl, P. Comparison of sedimentary PAHs in the rivers of Ammer (Germany) and Liangtan (China): Differences between early- and newly-industrialized countries. Environ. Sci. Technol. 2013, 47 (2), 701−709.
(2) Yan, Z. S.; Jiang, H. L.; Cai, H. Y.; Zhou, Y. L.; Krumholz, L. R. Complex interactions between the macrophyte Acorus Calamus and microbial fuel

cells during pyrene and benzo[a]pyrene degradation in sediments. Sci. Rep. 2015, 5, 10709. (3) Yan, Z. S.; Jiang, H. L.; Li, X. H.; Shi, Y. Accelerated removal of pyrene and benzo[a]pyrene in freshwater sediments with amendment of cyanobacteria-derived organic matter. J. Hazard. Mater. 2014, 272, 66−74. (4) Juhasz, A. L.; Naidu, R. Bioremediation of high molecular weight polycyclic aromatic hydrocarbons: a review of the microbial degradation of benzo[a]pyrene. Int. Biodeterior. Biodegrad. 2000, 45 (1−2), 57−88. (5) Kanaly, R. A.; Harayama, S. Biodegradation of high-molecularweight polycyclic aromatic hydrocarbons by bacteria. J. Bacteriol. 2000, 182 (8), 2059−2067. (6) DeBruyn, J. M.; Mead, T. J.; Wilhelm, S. W.; Sayler, G. S. PAH biodegradative genotypes in lake Erie sediments: evidence for broad geographical distribution of pyrene-degrading mycobacteria. Environ. Sci. Technol. 2009, 43 (10), 3467−3473. (7) Meckenstock, R. U.; Mouttaki, H. Anaerobic degradation of nonsubstituted aromatic hydrocarbons. Curr. Opin. Biotechnol. 2011, 22 (3), 406−414. (8) Hazen, T. C.; Dubinsky, E. A.; DeSantis, T. Z.; Andersen, G. L.; Piceno, Y. M.; Singh, N.; Jansson, J. K.; Probst, A.; Borglin, S. E.; Fortney, J. L.; Stringfellow, W. T.; Bill, M.; Conrad, M. E.; Tom, L. M.; Chavarria, K. L.; Alusi, T. R.; Lamendella, R.; Joyner, D. C.; Spier, C.; Baelum, J.; Auer, M.; Zemla, M. L.; Chakraborty, R.; Sonnenthal, E. L.; D'Haeseleer, P.; Holman, H. Y.; Osman, S.; Lu, Z.; Van Nostrand, J. D.; Deng, Y.; Zhou, J.; Mason, O. U. Deep-sea oil plume enriches indigenous oil-degrading bacteria. Science 2010, 330 (6001), 204−208. (9) Zhang, T.; Gannon, S. M.; Nevin, K. P.; Franks, A. E.; Lovley, D. R. Stimulating the anaerobic degradation of aromatic hydrocarbons in contaminated sediments by providing an electrode as the electron acceptor. Environ. Microbiol. 2010, 12 (4), 1011−20. (10) Yan, Z. S.; Song, N.; Cai, H. Y.; Tay, J. H.; Jiang, H. L. Enhanced degradation of phenanthrene and pyrene in freshwater sediments by combined employment of sediment microbial fuel cell and amorphous ferric hydroxide. J. Hazard. Mater. 2012, 199, 217−225. (11) Coates, J. D.; Anderson, R. T.; Woodward, J. C.; Phillips, E. J. P.; Lovley, D. R. Anaerobic hydrocarbon degradation in petroleumcontaminated harbor sediments under sulfate-reducing and artificially imposed iron-reducing conditions. Environ. Sci. Technol. 1996, 30 (9), 2784−2789. (12) Xu, M. Y.; Zhang, Q.; Xia, C. Y.; Zhong, Y. M.; Sun, G. P.; Guo, J.; Yuan, T.; Zhou, J. Z.; He, Z. L. Elevated nitrate enriches microbial functional genes for potential bioremediation of complexly contaminated sediments. ISME J. 2014, 8 (9), 1932−1944. (13) Morris, J. M.; Jin, S.; Crimi, B.; Pruden, A. Microbial fuel cell in enhancing anaerobic biodegradation of diesel. Chem. Eng. J. 2009, 146 (2), 161−167. (14) Lu, L.; Huggins, T.; Jin, S.; Zuo, Y.; Ren, Z. J. Microbial Metabolism and Community Structure in Response to Bioelectrochemically Enhanced Remediation of Petroleum HydrocarbonContaminated Soil. Environ. Sci. Technol. 2014, 48 (7), 4021−4029. (15) Wang, X.; Cai, Z.; Zhou, Q. X.; Zhang, Z. N.; Chen, C. H. Bioelectrochemical stimulation of petroleum hydrocarbon degradation in saline soil using U-tube microbial fuel cells. Biotechnol. Bioeng. 2012, 109 (2), 426−433. (16) Mohan, S. V.; Chandrasekhar, K. Self-induced bio-potential and graphite electron accepting

conditions enhances petroleum sludge degradation in bio-electrochemical system with simultaneous power generation. Bioresour. Technol. 2011, 102 (20), 9532−9541. (17) Yang, Y.; Zhang, N.; Xue, M.; Lu, S. T.; Tao, S. Effects of soil organic matter on the development of the microbial polycyclic aromatic hydrocarbons (PAHs) degradation potentials. Environ. Pollut. 2011, 159 (2), 591−595. (18) Luthy, R. G.; Aiken, G. R.; Brusseau, M. L.; Cunningham, S. D.; Gschwend, P. M.; Pignatello, J. J.; Reinhard, M.; Traina, S. J.; Weber, W. J.; Westall, J. C. Sequestration of hydrophobic organic contaminants by geosorbents. Environ. Sci. Technol. 1997, 31 (12), 3341−3347. (19) Cornelissen, G.; Gustafsson, O.; Bucheli, T. D.; Jonker, M. T. O.; Koelmans, A. A.; Van Noort, P. C. M. Extensive sorption of organic compounds to black carbon, coal, and kerogen in sediments and soils: Mechanisms and consequences for distribution, bioaccumulation, and biodegradation. Environ. Sci. Technol. 2005, 39 (18), 6881− 6895. (20) Fontaine, S.; Barot, S.; Barre, P.; Bdioui, N.; Mary, B.; Rumpel, C. Stability of organic carbon in deep soil layers controlled by fresh carbon supply. Nature 2007, 450 (7167), 277−280. (21) Hong, S. W.; Kim, H. S.; Chung, T. H. Alteration of sediment organic matter in sediment microbial fuel cells. Environ. Pollut. 2010, 158 (1), 185−191. (22) Song, T. S.; Yan, Z. S.; Zhao, Z. W.; Jiang, H. L. Removal of organic matter in freshwater sediment by microbial fuel cells at various external resistances. J. Chem. Technol. Biotechnol. 2010, 85 (11), 1489− 1493. (23) Plaza, C.; Xing, B.; Fernandez, J. M.; Senesi, N.; Polo, A. Binding of polycyclic aromatic hydrocarbons by humic acids formed during composting. Environ. Pollut. 2009, 157 (1), 257−263. (24) Ke, L.; Bao, W.; Chen, L.; Wong, Y. S.; Tam, N. F. Effects of humic acid on solubility and biodegradation of polycyclic aromatic hydrocarbons in liquid media and mangrove sediment slurries. Chemosphere 2009, 76 (8), 1102−1108. (25) Tejeda-Agredano, M. C.; Mayer, P.; Ortega-Calvo, J. J. The effect of humic acids on biodegradation of polycyclic aromatic hydrocarbons depends on the exposure regime. Environ. Pollut. 2014, 184, 435−442. (26) Smith, K. E. C.; Thullner, M.; Wick, L. Y.; Harms, H. Sorption to humic acids enhances polycyclic aromatic hydrocarbon biodegradation. Environ. Sci. Technol. 2009, 43 (19), 7205−7211. (27) Lovley, D. R.; Coates, J. D.; BluntHarris, E. L.; Phillips, E. J. P.; Woodward, J. C. Humic substances as electron acceptors for microbial respiration. Nature 1996, 382 (6590), 445−448. (28) Zhou, J. Z.; He, Z. L.; Yang, Y. F.; Deng, Y.; Tringe, S. G.; Alvarez-Cohen, L. High-throughput metagenomic technologies for complex microbial community analysis: open and closed formats. mBio 2015, 6 (1), e02288−14. (29) MacDonald, D. D.; Ingersoll, C. G.; Berger, T. A. Development and evaluation of consensus-based sediment quality guidelines for freshwater ecosystems. Arch. Environ. Contam. Toxicol. 2000, 39 (1), 20−31. (30) Song, T. S.; Jiang, H. L. Effects of sediment pretreatment on the performance of sediment microbial fuel cells. Bioresour. Technol. 2011, 102 (22), 10465−10470. (31) Zhou, J. Z.; Bruns, M. A.; Tiedje, J. M. DNA recovery from soils of diverse composition. Appl. Environ. Microbiol. 1996, 62 (2), 316− 322. (32) Zhou, J. Z.; Deng, Y.; Luo, F.; He, Z. L.; Tu, Q. C.; Zhi, X. Y.

Functional molecular ecological networks. mBio 2010, 1 (4), e00169-10−e00169-19. (33) Deng, Y.; Zhang, P.; Qin, Y.; Tu, Q.; Yang, Y.; He, Z.; Schadt, C. W.; Zhou, J. Network succession reveals the importance of competition in response to emulsified vegetable oil amendment for uranium bioremediation. Environ. Microbiol. 2016, 18 (1), 205−218. (34) Salinero, K. K.; Keller, K.; Feil, W. S.; Feil, H.; Trong, S.; Di Bartolo, G.; Lapidus, A. Metabolic analysis of the soil microbe Dechloromonas aromatica str. RCB: indications of a surprisingly complex life-style and cryptic anaerobic pathways for aromatic degradation. BMC Genomics 2009, 10, 351. (35) Lu, Z. M.; Deng, Y.; Van Nostrand, J. D.; He, Z. L.; Voordeckers, J.; Zhou, A. F.; Lee, Y. J.; Mason, O. U.; Dubinsky, E. A.; Chavarria, K. L.; Tom, L. M.; Fortney, J. L.; Lamendella, R.; Jansson, J. K.; D'Haeseleer, P.; Hazen, T. C.; Zhou, J. Z. Microbial gene functions enriched in the Deepwater Horizon deep-sea oil plume. ISME J. 2012, 6 (2), 451−460. (36) Sinsabaugh, R. L. Phenol oxidase, peroxidase and organic matter dynamics of soil. Soil Biol. Biochem. 2010, 42 (3), 391−404. (37) Xu, M. Y.; He, Z. L.; Zhang, Q.; Liu, J.; Guo, J.; Sun, G. P.; Zhou, J. Z. Responses of aromatic-degrading microbial communities to elevated nitrate in sediments. Environ. Sci. Technol. 2015, 49 (20), 12422−12431. (38) Widdel, F.; Rabus, R. Anaerobic biodegradation of saturated and aromatic hydrocarbons. Curr. Opin. Biotechnol. 2001, 12 (3), 259−276. (39) Kim, S. J.; Kweon, O.; Jones, R. C.; Freeman, J. P.; Edmondson, R. D.; Cerniglia, C. E. Complete and integrated pyrene degradation pathway in Mycobacterium vanbaalenii PYR-1 based on systems biology. J. Bacteriol. 2007, 189 (2), 464−472. (40) Liang, Y. T.; Van Nostrand, J. D.; Deng, Y.; He, Z. L.; Wu, L. Y.; Zhang, X.; Li, G. H.; Zhou, J. Z. Functional gene diversity of soil microbial communities from five oil-contaminated fields in China. ISME J. 2011, 5 (3), 403−413. (41) Hale, S. E.; Meynet, P.; Davenport, R. J.; Jones, D. M.; Werner, D. Changes in polycyclic aromatic hydrocarbon availability in River Tyne sediment following bioremediation treatments or activated carbon amendment. Water Res. 2010, 44 (15), 4529−4536. (42) Hennessee, C. T.; Li, Q. X. Effects of polycyclic aromatic hydrocarbon mixtures on degradation, gene expression, and metabolite production in four Mycobacterium species. Appl. Environ. Microbiol. 2016, 82 (11), 3357−3369. (43) Neumann, D.; Heuer, A.; Hemkemeyer, M.; Martens, R.; Tebbe, C. C. Importance of soil organic matter for the diversity of microorganisms involved in the degradation of organic pollutants. ISME J. 2014, 8 (6), 1289−1300. (44) Collins, P. J.; Kotterman, M.; Field, J. A.; Dobson, A. Oxidation of anthracene and benzo[a]pyrene by Laccases from Trametes versicolor. Appl. Environ. Microbiol. 1996, 62 (12), 4563−4567. (45) Hadibarata, T.; Kristanti, R. A. Fate and cometabolic degradation of benzo[a]pyrene by white-rot fungus Armillaria sp. F022. Bioresour. Technol. 2012, 107, 314−318. (46) Holman, H. Y.; Nieman, K.; Sorensen, D. L.; Miller, C. D.; Martin, M. C.; Borch, T.; McKinney, W. R.; Sims, R. C. Catalysis of PAH biodegradation by humic acid shown in synchrotron infrared studies. Environ. Sci. Technol. 2002, 36 (6), 1276−1280. (47) Bittner, M.; Macikova, P.; Giesy, J. P.; Hilscherova, K. Enhancement of AhR-mediated activity of selected

pollutants and their mixtures after interaction with dissolved organic matter. Environ. Int. 2011, 37 (5), 960−964. (48) Roden, E. E.; Kappler, A.; Bauer, I.; Jiang, J.; Paul, A.; Stoesser, R.; Konishi, H.; Xu, H. F. Extracellular electron transfer through microbial reduction of solid-phase humic substances. Nat. Geosci. 2010, 3 (6), 417−421. (49) Reimers, C. E.; Alleau, Y.; Bauer, J. E.; Delaney, J.; Girguis, P. R.; Schrader, P. S.; Stecher, H. A. Redox effects on the microbial degradation of refractory organic matter in marine sediments. Geochim. Cosmochim. Acta 2013, 121, 582−598. (50) Lu, L.; Yazdi, H.; Jin, S.; Zuo, Y.; Fallgren, P. H.; Ren, Z. J. Enhanced bioremediation of hydrocarbon-contaminated soil using pilot-scale bioelectrochemical systems. J. Hazard. Mater. 2014, 274, 8− 15. (51) Li, X. J.; Wang, X.; Zhang, Y. Y.; Zhao, Q.; Yu, B. B.; Li, Y. T.; Zhou, Q. X. Salinity and conductivity amendment of soil enhanced the bioelectrochemical degradation of petroleum hydrocarbons. Sci. Rep. 2016, 6, 32861. (52) Mao, D. Q.; Lu, L.; Revil, A.; Zuo, Y.; Hinton, J.; Ren, Z. J. Geophysical monitoring of hydrocarbon-contaminated soils remediated with a bioelectrochemical system. Environ. Sci. Technol. 2016, 50 (15), 8205−8213.